Molecular Biology of the Cell
Vol. 14, 1097–1108, March 2003

Polarized Distribution of IQGAP Proteins in Gastric Parietal Cells and Their Roles in Regulated Epithelial Cell Secretion

Rihong Zhou*†‡ Zhen Guo,*† Charles Watson,‡ Emily Chen,‡ Rong Kong,† Wenxian Wang,† and Xuebiao Yao†‡§

†Laboratory of Cell Dynamics, School of Life Sciences, University of Science and Technology of China, Hefei, China 230027; and ‡Department of Molecular and Cell Biology, University of California, Berkeley, California 94720

Submitted July 24, 2002; Revised October 30, 2002; Accepted November 22, 2002
Monitoring Editor: Keith Mostov

Actin cytoskeleton plays an important role in the establishment of epithelial cell polarity. Cdc42, a member of Rho GTPase family, modulates actin dynamics via its regulators, such as IQGAP proteins. Gastric parietal cells are polarized epithelial cells in which regulated acid secretion occurs in the apical membrane upon stimulation. We have previously shown that actin isoforms are polarized to different membrane domains and that the integrity of the actin cytoskeleton is essential for acid secretion. Herein, we show that Cdc42 is preferentially distributed to the apical membrane of gastric parietal cells. In addition, we revealed that two Cdc42 regulators, IQGAP1 and IQGAP2, are present in gastric parietal cells. Interestingly, IQGAP2 is polarized to the apical membrane of the parietal cells, whereas IQGAP1 is mainly distributed to the basolateral membrane. An IQGAP peptide that competes with full-length IQGAP proteins for Cdc42-binding in vitro also inhibits acid secretion in streptolysin-O-permeabilized gastric glands. Furthermore, this peptide disrupts the association of IQGAP and Cdc42 with the apical actin cytoskeleton and prevents the apical membrane remodeling upon stimulation. We propose that IQGAP2 forms a link that associates Cdc42 with the apical cytoskeleton and thus allows for activation of polarized secretion in gastric parietal cells.

INTRODUCTION

Rho GTPases are members of Ras superfamily of monomeric 20- to 30-kDa GTP-binding proteins (Hall, 1998). Cdc42 is one of the well-characterized small GTPases among the Ras superfamily and is implicated in a variety of cellular functions, including the establishment of cell polarity (Drubin and Nelson, 1996). Cdc42 acts as a molecular switch, cycling between an active GTP-bound and an inactive GDP-bound state. In the GTP-bound form, it interacts with effector molecules to trigger the downstream signaling cascade, whereas its intrinsic GTPase activity returns Cdc42 to the GDP-bound form and terminates the downstream signaling.

Recent studies show that Cdc42 interacts with exocyst via a direct association with Sec3 and is involved in yeast secretion (Guo *et al.*, 1999; Zhang *et al.*, 2001). Cdc42 also interacts with IQGAP proteins, a group of 175- to 185-kDa proteins that received their names from their IQ domains and a region with sequence similarity to the catalytic domain of RAS-GAPs (Weissbach *et al.*, 1994). IQGAP1 contains four IQ motifs, a calponin homology domain, a WW domain (containing conserved tryptophan residues), and a Ras-GAP homology domain (Hart *et al.*, 1996). It has been shown that WW domain functions as a pSer/Thr-Pro-binding module integrating kinase activity with downstream signaling cascade (Verdecia *et al.*, 2000). IQGAP2 is a 175-kDa protein initially found in rat liver (McCallum *et al.*, 1996). Like IQGAP1, IQGAP2 has one N-terminal calponin homology motif, one WW domain, four IQ motifs, and one Ras-GAP homology domain. It was reported that IQGAP2 has a tissue-specific expression profile, being enriched in liver. Several proteins, such as Cdc42 (Kuroda *et al.*, 1996; Joyal *et al.*, 1997), actin, and calmodulin, bind to IQGAP1 and IQGAP2. IQGAP1 has been detected in a complex with F-actin and Cdc42, which is disrupted by dominant negative Cdc42 protein (Erickson *et al.*, 1997). However, it is unknown how

Article published online ahead of print. Mol. Biol. Cell 10.1091/mbc.E02–07–0425. Article and publication date are at www.molbiolcell.org/cgi/doi/10.1091/mbc.E02–07–0425.

* These authors contributed equally to this work.
§ Corresponding author. E-mail address: xbyao@uclink4.berkeley.edu.

IQGAP proteins interact with Cdc42 and exert their physiological functions.

Cdc42 undergoes conformational changes upon binding to GTP (Hall, 1998; Feig, 1999). The constitutively active form of Cdc42 protein contains a glutamine to leucine substitution at amino acid 61, which prevents the GAP-stimulated GTPase activity of Cdc42, resulting in a protein that is always in the active, GTP-bound, state. The dominant negative Cdc42 involves the mutation of a threonine to asparagine at amino acid 17, which stabilizes the GDP-bound form of the protein, resulting in an inactive form of Cdc42 protein. Cycling between GTP- and GDP-bound Cdc42 is regulated by numerous cellular proteins, including IQGAP1 and IQGAP2 (Hall, 1998; Bishop and Hall, 2000). Over the years, these mutant forms of Cdc42 have provided a powerful tool to modulate the activity of Cdc42 protein and dissect the downstream signaling events (Feig, 1999).

Gastric parietal cells are polarized epithelial cells in which hydrochloric acid secretion is triggered by the paracrine, endocrine, and neurocrine pathways (Forte and Yao, 1996; Yao and Forte, 2003). The physiological stimuli include histamine, gastrin, and acetylcholine via their receptors located on the basolateral plasma membranes. Stimulation of acid secretion typically involves an initial elevation of intracellular calcium and cAMP followed by activation of the cAMP-dependent protein kinase cascade, which in turn triggers the translocation and insertion of the proton pump enzyme H^+, K^+-ATPase into apical plasma membranes of parietal cells, resulting in a dramatic remodeling of the apical membrane cytoskeleton (Forte *et al.*, 1977, 1981). Therefore, acid secretion in parietal cells provides a model system to study cAMP-coupled polarized secretion (Chew, 1985; Yao and Forte, 2003).

Genetic studies indicate that elimination of IQGAP1 does not affect overall development of the mouse but causes an aberrant epithelial cell growth in the stomach (Li *et al.*, 2000), suggesting that Cdc42*IQGAP1 interaction functions in gastric epithelial cells. It was of great interest to determine whether aberrant cell growth affects polarized secretion in gastric parietal cells. To understand this, we probed for the distribution of Cdc42 in the parietal cells and discovered that Cdc42 is located to the apical membrane. Addition of dominant negative Cdc42 protein into streptolysin O-permeabilized cells prevents the activation of gastric parietal cells, indicating that Cdc42 function is necessary for the secretion. Because our pull-down assay showed that both IQGAP1 and IQGAP2 associate with active Cdc42, we probed for their distribution in parietal cells. Interestingly, IQGAP2 is mainly distributed to the apical membrane, whereas IQGAP1 is located to the basolateral membrane of parietal cells. Using an inhibitory peptide that disrupts the IQGAP*Cdc42 interaction, we demonstrated the importance of such an interaction in the apical membrane cytoskeletal dynamics associated with secretion. Our studies suggest that IQGAP2 may provide a molecular linker between Cdc42 and the actin cytoskeleton in polarized epithelial cell secretion.

MATERIALS AND METHODS

Materials and Chemicals

Anti-Cdc42 antibody was purchased from Santa Cruz Biotechnology (Santa Cruz, CA), whereas IQGAP1 and IQGAP2 antibodies were obtained from Upstate Biotechnology (Lake Placid, NY). The bacterial expression vectors containing constitutively active and dominant negative Cdc42 fused to glutathione *S*-transferase (GST) were generous gifts from Dr. Alan Hall (University College of London, London, United Kingdom).

Purification of Recombinant Cdc42 Proteins

Constitutively active and dominant negative Cdc42 were expressed in *Escherichia coli.* BL21 and the purification of GST fusion proteins by using glutathione-Sepharose beads was carried out as described previously (Ammar *et al.*, 2002). Briefly, 1 liter of LB media was inoculated with bacteria transformed with either constitutive active GST-Cdc42 (CA Cdc42) or dominant negative GST-Cdc42 (DN Cdc42). The expression of protein was induced by addition of 0.5 mM isopropyl β-D-thiogalactopyranoside. Bacteria were harvested by centrifugation 3 h after the induction, resuspended in phosphate-buffered saline (PBS) containing proteinase inhibitors (leupeptin, pepstatin, and chymostatin; 5 μg/ml), and sonicated for four bursts of 10 s each by using a probe-tip sonicator. The lysis solution was cleared of insoluble material by centrifugation for 20 min at 10,000 × *g*. The soluble fraction was applied to a column packed with glutathione-agarose beads, followed by extensive washes with PBS.

For assaying their activities in parietal cell secretion, the GST-Cdc42 proteins were subject to thrombin cleavage to release Cdc42 from the GST tag. Exchange of media was achieved using a desalting column (Econ-*Pac*I0 DG; Bio-Rad, Hercules, CA). The fusion protein in K-buffer was estimated to be 90% pure by SDS-PAGE; major contaminates were degraded fragments of Cdc42 proteins. Protein concentrations were determined by Bradford assay (Ammar *et al.*, 2002).

Isolation and Culture of Gastric Parietal Cells

Primary culture of gastric parietal cells from rabbit was maintained as described previously (Ammar *et al.*, 2002). Briefly, the perfused rabbit gastric mucosa was collected, minced, and digested with 0.125 mg/ml collagenase (Sigma-Aldrich, St. Louis, MO) in minimal essential medium (containing 20 mM HEPES, pH 7.4). The dispersed cells were strained and washed three times with minimal essential medium-HEPES and subjected to treatment of amphotericin B (25 μg/ml; Sigma-Aldrich) in medium B (DMEM/F-12 [Invitrogen, Carlsbad, CA] supplemented with 20 mM HEPES, 0.2% bovine serum albumin, 10 mM glucose, 8 nM epidermal growth factor, 1× selenite, insulin, and transferrin medium [Sigma-Aldrich], 1 mM glutamine, 100 U/ml penicillin-streptomycin, 400 μg/ml gentamicin sulfate, and 15 μg/l geneticin or 20 μg/ml novobiocin, pH 7.4) to prevent yeast infection. Treated cells were then plated onto Matrigel (Collaborative Research, Bedford, MA)-coated coverslips and incubated at 37°C in medium B (minus amphotericin B).

Assay for Acid Secretion by Using Permeabilization of Gastric Glands

Gastric glands were permeabilized using streptolysin-O (SLO) as described by Ammar *et al.* (2002). In brief, SLO-glands were resuspended in K-buffer (10 mM Tris base, 20 mM HEPES acid, 100 mM KCl, 20 mM NaCl, 1.2 mM $MgSO_4$, 1 mM NaH_2PO_4, and 40 mM mannitol, pH 7.4) containing 1 mM pyruvate and 10 mM succinate and then incubated with different amount of CA Cdc42 and DN Cdc42 proteins at 37°C for assaying their abilities to modulate acid secretion. To validate the functional importance of Cdc42*IQGAP interactions in parietal cell activation, we also used an IQGAP-derived synthetic peptide (GNPTVIKM) based on the Cdc42-binding motif on IQGAP1 and verified by a recent mutational analysis (Brill *et al.*, 1996; Fukata *et al.*, 2002). The peptide was introduced into SLO-glands for assessing its ability to modulation parietal cell

secretion. A scrambled sequence (GMKTVINP) of this peptide was used as a control.

Stimulation of intact or SLO-permeabilized gastric glands was quantified using the aminopyrine (AP) uptake assay as described by Yao *et al.* (1993, 1996b). Briefly, SLO-glands were kept in the resting state with cimetidine (100 μM) or stimulated with cAMP (100 μM) plus ATP (1 mM). The effect of these Cdc42 proteins on acid secretion was judged by [^{14}C]AP uptake that was calculated as the ratio of intracellular/extracellular as described previously (Yao *et al.*, 1993).

Pull-Down Experiments

The GST-fusion proteins on the Sepharose beads were used as affinity matrix to isolate proteins interacting with Cdc42 by using the soluble fraction from gastric epithelial cells as described previously (Yao *et al.*, 1996a). Briefly, the GST-Cdc42 (both CA and DN) bound Sepharose beads were incubated with the gastric soluble fraction for 2 h at 4°C. After the incubation, the beads were extensively washed with PBS and boiled in SDS-PAGE sample buffer. The Cdc42 proteins and their binding proteins were separated on ~6–16% gradient SDS-PAGE gel and visualized using Coomassie Blue staining. Interesting bands were removed and subject to in-gel digestion with trypsin as described by Zhang *et al.* (2002).

To test whether the IQGAP peptide disrupts Cdc42*IQGAP interactions, gastric IQGAP proteins bound GST-Cdc42 affinity beads were incubated with 10 μg/ml IQGAP peptide for 30 min at room temperature. The affinity beads were then collected and boiled in SDS-PAGE sample buffer, whereas the proteins bound were subject to SDS-PAGE.

In-Gel Digestion

In-gel digestion was a modification of the method of Rosenfeld *et al.* (1992). Protein bands (~0.3 μg) were excised and minced using a new razor blade, and the pieces were destained with three washes of 50% Acn-25 mM NH_4HCO_3 (~10 min each). The destained gel pieces were dried in a Speedvac vacuum, followed by rehydration in 50 μl of 25 mM NH_4HCO_3, pH 8.0, that included 0.01 μg/ml trypsin. The pieces were overlaid with 50 μl of 25 mM NH_4HCO_3 and incubated for 15 h at 37°C. Peptides were recovered by three extractions of the digestion mixture with 50% Acn-5% trifluoroacetic acid. All supernatants were pooled and concentrated to 5 μl in a Speedvac and brought back up to 25 μl in 50% Acn-5% trifluoroacetic acid. The peptide mix was stored at 20°C until further analysis.

Matrix-assisted Laser Desorption Ionization/Time of Flight (MALDI-TOF) Mass Spectrometry of Cdc42-binding Protein Peptides

Aliquots of unseparated tryptic digests were cocrystallized with cyano-4-hydroxycinnamic acid and analyzed using a MALDI delayed-extraction reflectron TOF instrument (Voyager Elite mass spectrometer; Applied Biosystems, Foster City, CA) equipped with a nitrogen laser. Measurements were performed in a positive ionization mode. All MALDI spectra were externally calibrated using a standard peptide mixture. Some postsource-decay spectra were acquired on a TofSpec SE MALDI-TOF mass spectrometer (Micromass, Manchester, United Kingdom) with a nitrogen laser and operated in the reflectron mode.

Database Searches for Protein Identification

Database interrogations based on experimentally determined peptide masses were carried out using mass spectrometry (MS)-Fit. Postsource-decay data interrogation was performed using MS-Tag. Both software programs were developed in the University of California, San Francisco, MS Facility and are available at http://prospector.ucsf.edu. Both the National Center for Biotechnology Information protein database and Swiss Prot database were searched. Search parameters included the putative protein molecular weight and a peptide mass tolerance of 100–200 parts per million.

Immunofluorescence Microscopy

For localization of Cdc42 and IQGAP proteins, cultured parietal cells were fixed with 2% formaldehyde for 10 min. After fixation, cells were washed three times followed by permeabilization in 0.1% Triton X-100 for 5 min. To test for the possible relocation of Cdc42 and IQGAP proteins associated with the acid secretion, aliquots of the cells were treated with 100 μM histamine plus 50 μM 3-isobutyl-1-methylxanthine with or without SCH28080, a proton pump inhibitor (Agnew *et al.*, 1999) kindly provided by Dr. J.G. Forte (University of California, Berkeley, CA).

To evaluate effects of the IQGAP peptide on Cdc42*IQGAP interactions in vivo, the peptide is covalently fused to the TAT peptide (YGRKKRRQRRRG) to retain the chimeric peptide membrane permeability (Chen *et al.*, 1999). The inhibitory effect of the TAT-fused peptide on acid secretion of intact cells was found to be equal to that of the peptide on SLO-permeabilized cells as judged by AP uptake assay. The efficiency of the peptide across the cell membrane was assessed under a fluorescence microscopy to monitor the uptake of fluorescein-isothiocyanate–labeled peptide. The TAT-fused peptide uptake efficiency in the parietal cells was typically 83 $\pm$ 4% as judged by the cytoplasmic accumulation of the fluorescein.

To evaluate the TAT-fused peptide on the apical membrane remodeling associated with the secretion, the parietal cells were pretreated with 10 μg/ml peptide for 5 min followed by the treatment of histamine plus 3-isobutyl-1-methylxanthine with and without SCH28080. A scrambled sequence of this peptide fused to TAT was used as a control. After the treatment, the cells were then fixed and permeabilized as described above.

The fixed and permeabilized cells were blocked in 1% bovine serum albumin in phosphate-buffered saline (PBS) for 15 min followed by a 60-min incubation with the primary antibodies to Cdc42, IQGAP1, IQGAP2, and ezrin, respectively. The primary antibodies were then visualized by a fluorescein isothiocyanate (FITC)-conjugated goat anti-mouse IgG (Jackson Immunoresearch Laboratories, West Grove, PA) in a 20-min subsequent incubation. Actin was detected by coincident incubation with 80 nM rhodamine-labeled phalloidin. Coverslips were supported on slides by grease pencil markings and mounted in Vectorshield (Vector Laboratories, Burlingame, CA). Images were taken on an Axiovert 200 fluorescence microscope (Carl Zeiss, Jena, Germany) by using a 63 $\times$ 1.3 numerical aperture PlanApo objective. Figures were constructed using Adobe Photoshop (Adobe Systems, Mountain View, CA).

Confocal Microscopy

Immunostained parietal cells were examined under a laser-scanning confocal microscope LSM510 NLO (Carl Zeiss) scan head mounted transversely to an inverted microscope (Axiovert 200; Carl Zeiss) with a 40 $\times$ 1.3 numerical aperture PlanApo objective. Single images were collected by average of 10 scans at a scan rate of four scan/s. Optical section series were collected with a spacing of 0.4 μm in the z-axis through the ~12-μm thickness of the cultured parietal cells. The images from double labeling were simultaneously collected using a dichroic filter set with Zeiss image processing software (LSM 5, Carl Zeiss). Digital data were exported into Adobe Photoshop for presentation.

Measurement of Diameter of Apical Vacuoles

The diameter of apical valcuoles was measured using LSM 5 software (Carl Zeiss), phalloidin-marked vacuoles, and an Axiovert 200 fluorescent microscope calibrated with a stage micrometer. When suitable vacuoles were identified, the image was enlarged threefold to facilitate accurate placement of a computer-generated cursor over

the center of each vacuole. Only the circular vacuoles that were in the same focal plane were measured.

Detergent Extraction of Cultured Parietal Cells and Assay of Cdc42 and IQGAP2 Content

To determine whether the TAT-fused peptide disrupts the Cdc42*IQGAP interactions with the cytoskeleton, gastric parietal cells were treated with the TAT-fused peptide for 10 min at 37°C followed by detergent extraction with the protocol described by Yao *et al.* (1997). Briefly, the parietal cells, both TAT-fused peptide treated and its control, were exposed to cytoskeleton stabilization buffer (100 mM PIPES, 20 mM HEPES, pH 7.3, 5 mM EGTA, 2 mM $MgCl_2$, and 4 M glycerol) containing 0.1% Triton X-100 for 2 min at room temperature followed by centrifugation to separate Triton X-100–soluble from Triton X-100–insoluble fraction. The proteins in both fractions were first precipitated with cold methanol and then solubilized in SDS-PAGE sample buffer. Equal proportions of materials from various fractions were loaded onto SDS-PAGE gels followed by transferring the separate proteins onto nitrocellulose membranes. The membranes were then subject to Western blotting by using antibodies reacting with ezrin, Cdc42, IQGAP1, and IQGAP2, respectively.

Western Blot

Samples were subject to SDS-PAGE on ~6–16% gradient gel and transferred onto nitrocellulose membrane. Proteins were probed by appropriate primary antibodies and detected using enhanced chemiluminescence (Pierce Chemical, Rockford, IL). The band intensity was then quantified using a PhosphorImager (Amersham Biosciences, Piscataway, NJ).

RESULTS

Cdc42 Is Primarily Localized to Apical Plasma Membrane of Resting and Secreting Gastric Parietal Cells

To test for the presence of Cdc42 in gastric glandular cells, we carried out Western blotting analysis by using a monoclonal antibody (mAb) to Cdc42. Glandular cell lysates were subjected to SDS-PAGE with subsequent transblotting onto a nitrocellulose membrane. The mAb recognized a 27-kDa protein from whole glandular cell lysates, indicating that Cdc42 is present in gastric glandular cells (our unpublished data). Given the heterogeneity of gastric glandular cells, however, it was difficult to judge whether Cdc42 is in fact present in gastric parietal cells or other glandular cells such as chief cells. To distinguish these cases, we pursued immunofluorescence staining of Cdc42 in cultured parietal cells.

Previous studies of gastric glands demonstrated that ezrin and the β-actin isoform in parietal cells were predominately expressed with primary distribution to the apical canalicular membrane with less intense staining to the basolateral surface (Yao *et al.*, 1995, 1996a), indicating the polarized distribution profile present in some actin cytoskeletal proteins. To ascertain the localization of Cdc42 in relation to the actin cytoskeleton in parietal cells, we carried out confocal microscopic analyses of double immunofluorescence staining of Cdc42 and F-actin in cultured parietal cells (Yao *et al.*, 1995; Agnew *et al.*, 1999).

To probe for the spatial distribution profile of Cdc42, we took serial confocal images from double-stained cultured parietal cells over the full thickness of the cells (12–15 μm) with a z-axis spacing of 0.4 μm. Figure 1A shows a series of optical sections taken from cells simultaneously probed with fluorescein-labeled anti-Cdc42 antibody and rhodamine-conjugated phalloidin. For simplicity, the figure includes only every fifth section from the series taken from the bottom to the top of the cells. In the central region of the cell (Fig, 1A, b–g and b′–g′), Cdc42 staining is clearly visible as rings outlining the apical canalicular membrane. Within parietal cells, Cdc42 and F-actin are primarily colocalized to the ring-like apical canalicular membrane invaginated into the cytoplasm of parietal cells, but a very light deposition of stain indicates their presence at the basolateral surface. Colocalization of Cdc42 with F-actin in the canalicular membrane is evidenced as the focal plane moves up and down through the cell. In fact, the overlapping images (yellow, a″–g″) verify the superimposition of the two stains in the apical plasma membrane of parietal cells.

Stimulation of parietal cells with histamine results in dramatic extension of the apical canalicular plasma membrane due to insertion of H^+,K^+-ATPase–containing vesicular membranes and subsequent proton pumping into the canalicular space (Agnew *et al.*, 1999). Because of this swelling, stimulated parietal cells are considerably larger in diameter than their resting counterpart (Agnew *et al.*, 1999). This is consistent with the morphological and functional transition of parietal cells in intact tissue where active HCl and water transport occurs at secretion (Forte *et al.*, 1977; Helander and Sundell, 1984). To test whether the stimulation affects localization of Cdc42 relative to the actin cytoskeleton, we carried out immunofluorescence staining of stimulated parietal cells. Figure 1B shows a series of optical sections taken from secreting parietal cells simultaneously probed with fluorescein-labeled anti-Cdc42 antibody and rhodamine-conjugated phalloidin. The dilated apical canalicular membrane occupies most of the cytoplasmic space. Similar to Figure 1A, only every fifth section from the series was taken. F-actin labeling (Figure 1B, a′–h′) outlines the dilated apical membrane in addition to some basolateral surface staining. As within resting parietal cells, Cdc42 and F-actin are primarily colocalized to the same regions in secreting cells. Colocalization of Cdc42 with F-actin is readily apparent as the focal plane moves through the cell. Thus, Cdc42 remains associated with actin cytoskeleton at the apical plasma membrane in secreting parietal cells.

Cdc42 Participates in Stimulus-coupled, Polarized Secretion in Parietal Cells

It has been shown that the active form of Cdc42 can trigger actin dynamics, mimicking hormone stimulation in fibroblasts (Hall. 1998). Because Cdc42 is associated with actin cytoskeleton of apical membrane, where cytoskeletal dynamics is coupled to acid secretion (Yao *et al.*, 1995, 1996a), we sought to test for the possible role of Cdc42 in gastric acid secretion by using our newly developed permeabilized gastric gland model (Ammar *et al.*, 2002). Thus, we introduced active and negative Cdc42 proteins into SLO-glands and tested their ability to modulate acid secretion. Addition of 100 μM cAMP and ATP stimulates gastric acid secretion in SLO-glands reflected by a typical 10-fold increase in AP uptake ratio (Figure 2; cAMP + ATP; hatched bar), as reported previously (Ammar *et al.*, 2002). Addition of active Cdc42 protein (~1–25 μg/ml) in the presence of cAMP plus ATP caused a slight but insignificant increase of AP uptakes

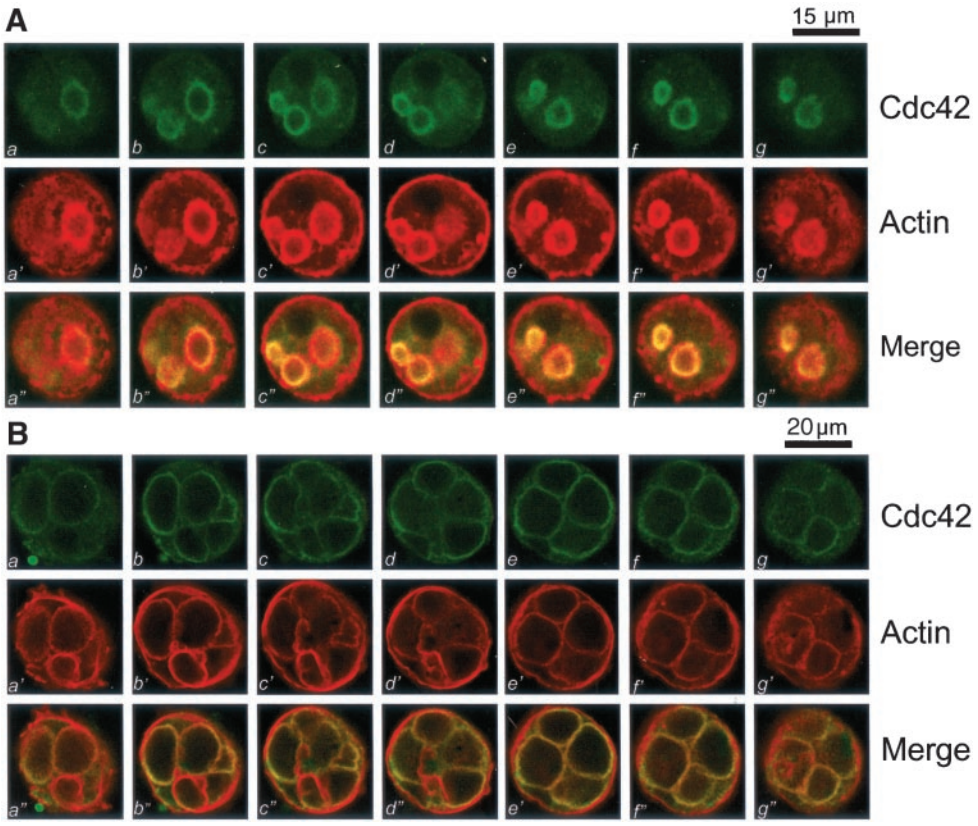

Figure 1. Cdc42 is primarily located to the apical plasma membrane of resting and secreting gastric parietal cells. Cultured gastric parietal cells were prepared as described in MATERIALS AND METHODS. The cultured cells were either maintained in 100 μM cimetidine for resting (A) or treated with 100 μM histamine plus SCH28080 (B) for 20 min before fixation. Fixed and permeabilized cells were incubated with a Cdc42 mAb followed by an FITC-conjugated goat anti-mouse IgG. The cells were also counterstained with rhodamine-labeled phalloidin to visualize filamentous actin cytoskeleton of the cells. Individual fluorescent images from two fluorophores were collected and presented using Adobe Photoshop. (A) This triple montage represents a series of optical sections, spaced ~0.4 μm in the z-axis, from the bottom (a, a′ and a″) to the top (g, g′, and g″), of a resting parietal cell doubly stained for Cdc42 (green, a–g), F-actin (red, a′–g′), and their merges (a″–g″). Cdc42 is chiefly localized to the intracellular of parietal cells, with a distribution profile similar to that F-actin, except for the basolateral surface staining of F-actin. Bar, 15 μm. (B) This triple montage of a series of optical sections was arranged in a similar way to that of A, but in this case the parietal cells were stimulated with histamine. Cdc42 remains localized to the apical plasma membrane of secreting cells in addition to cytoplasmic staining. The distribution of Cdc42 to apical plasma membrane is superimposed to that of F-actin staining. Bar, 20 μm.

(cross bars). However, addition of DN Cdc42 protein into SLO-glands resulted in a dose-dependent suppression of acid secretion, reaching 42% inhibition when DN Cdc42 protein was added at 25 μg/ml (Figure 2, spotted bars). This assay suggested that activation of Cdc42 protein is involved in parietal cell activation. However, addition of active Cdc42 protein in the absence of cAMP plus ATP did not trigger acid secretion in SLO-glands (our unpublished data), implying that activation of Cdc42 is important but alone is not sufficient for an active parietal cell secretion.

Identification of Cdc42-binding Proteins in Gastric Epithelial Cells

Because active Cdc42 plays a role in parietal cell activation, we sought to identify the proteins interacting with active Cdc42. To this end, we expressed both CA and DN GST-Cdc42 proteins in bacteria and made affinity Sepharose beads. As shown in Figure 3A, the GST fusion proteins on the Sepharose beads migrated on SDS-PAGE gel as a single band with apparent molecular mass of 47 kDa. Incubation of gastric cell lysates with active (but not inactive) GST-Cdc42 protein beads resulted in retention of two high-molecular-weight proteins to the affinity beads (Figure 3A; marked as IQGAP1 and IQGAP2). These two bands were specifically absorbed by the active Cdc42 protein; negative Cdc42 did not retain these two proteins. To reveal the identities of these two proteins, we removed each of the two protein bands from the Coomassie Blue-stained gel and carried out in-gel digestion by using trypsin. The resulting peptides were analyzed using a MALDI-TOF mass spectrometer. It was then apparent that a large number of the peptide signals contributed by both IQGAP1 and IQGAP2 showed a statistically significant match. The MALDI-TOF MS peptide mass spectra indicated that IQGAP1 and IQGAP2 are specifically bound to active Cdc42 protein.

The identification of IQGAP1 and IQGAP2 as active Cdc42-binding partners by MALDI-TOF MS was then confirmed by Western blotting with isoform-specific monoclonal antibodies to IQGAP1 and IQGAP2, respectively (Figure 3C). Western blots of proteins from the same experiment verified that IQGAP1 and IQGAP2 are bound to Cdc42 in an activity-dependent manner. Neither protein was detected in the control pull-down assay by using negative Cdc42 protein. To validate the specificity of our pull-down assay, we also carried out Western blotting of ezrin by using 4A5 mAb to detect the presence of ezrin in the Cdc42 pull-down. As shown in Figure 4C, ezrin was not associated with either active or negative Cdc42 protein, indicating a specific asso-

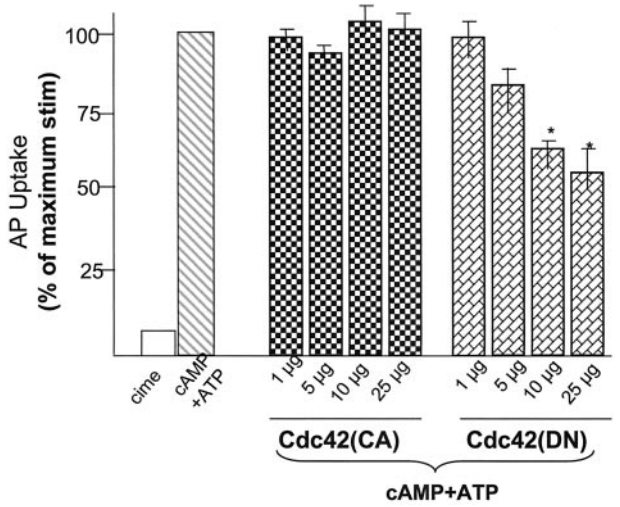

Figure 2. Cdc42 participates in acid secretion in SLO-permeabilized gastric glands. Recombinant Cdc42, both constitutive active and dominant negative, proteins were purified from bacteria and added into SLO-gland suspensions as indicated amount (micrograms per milliliter). Glands were then stimulated with 100 μM cAMP plus 100 μM ATP, and the AP uptake was measured as described in MATERIALS AND METHODS. AP data are plotted as percentage of the stimulated control for each of experiment. Error bars as percentage of the stimulated control for each experiment. Error bars represent SE; n = 5. *, significant difference from stimulated controls ($p < 0.05$).

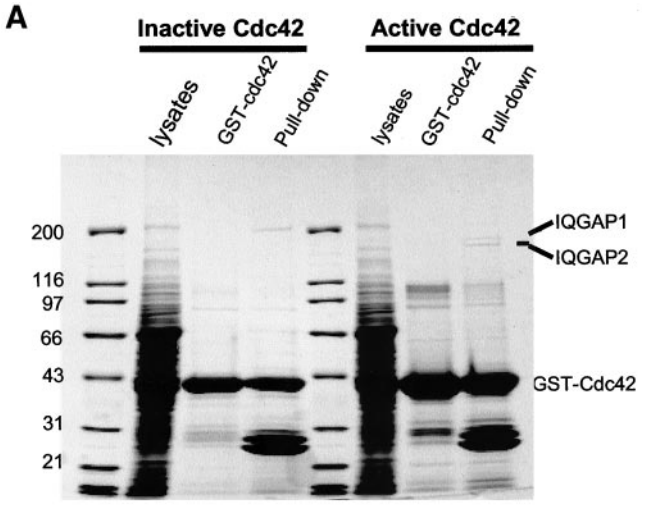

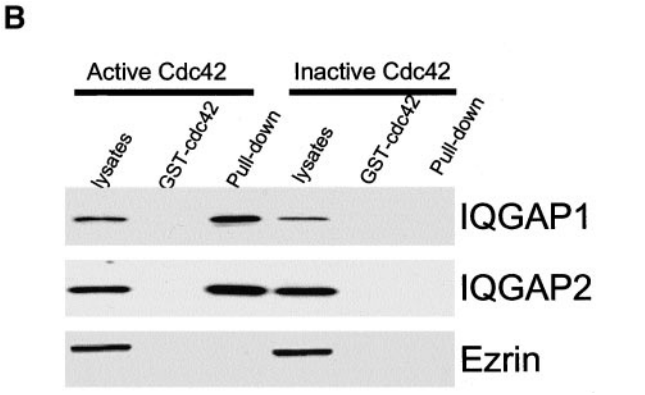

Figure 3. Identification of IQGAP1 and IQGAP2 as major Cdc42-binding proteins in gastric epithelial cells. (A) Cdc42 pulls down two major high-molecular-weight polypeptides from gastric lysates. Constitutive active and dominant negative GST-cdc42 proteins coupled to glutathione agarose beads were loaded with lysates of gastric epithelial cells. Bound proteins were fractionated by SDS-PAGE and stained with Coomassie Blue. Note there are two polypeptides with approximate molecular mass of 175 and 185 kDa, respectively. (B) Validation of mass spectrometric analyses of IQGAP1 and IQGAP2. A duplicate of SDS-PAGE gel of A was used for transblotting. The blot was used for probing IQGAP1, IQGAP2, and ezrin by using three different monoclonal antibodies, respectively. Western blotting analyses confirmed that IQGAP1 and IQGAP2, but not ezrin, were pulled down by constitutive active Cdc42 protein.

ciation between active Cdc42 and the IQGAP proteins. These data also indicate that both IQGAP1 and IQGAP2 are present in gastric epithelial cells.

IQGAP1 Is Mainly Localized to Basolateral Membrane of Parietal Cells

Because Cdc42 is present in parietal cells and associates with both IQGAP1 and IQGAP2 in a binding assay, we sought to define the respective subcellular localization of IQGAP1 and IQGAP2 in cultured parietal cells, which provide very interesting morphology of polarity. To probe for the precise spatial distribution of IQGAP1, we took serial confocal images from double-stained cultured parietal cells over the full thickness of the parietal cells. Figure 4A shows a series of optical sections taken from cultured parietal cells simultaneously probed with fluorescein-labeled anti-IQGAP1 mAb and rhodamine-conjugated phalloidin. In general, the F-actin staining shown in Figure 4A is consistent with what was observed in the previous figures. However, the optical sections shown in Figure 4A (a–g vs. a′–g′) reveal a significant difference in the pattern of F-actin staining and IQGAP1 staining. Overall, there was very little overlap in the distribution of F-actin and IQGAP1 near the apical plasma membrane. However, there was some colocalization of F-actin with IQGAP1 toward the basolateral surfaces of parietal cells (Figure 4A, c–e vs. c′–e′). As noted above, F-actin is mainly localized to the circular vacuoles suggestive of the invaginated apical membrane. Staining of IQGAP1 is heavily localized to the basolateral surface with some suggestive colocalization with F-actin in the regions immediately adjacent to that surface.

To test whether stimulation affects localization of IQGAP1 related to the actin cytoskeleton during parietal cell activation, we carried out immunofluorescence staining of stimulated parietal cells. As shown in Figure 1B, stimulation induced dilation of the apical canalicular membrane that occupies most of the cytoplasmic space of the parietal cells. Figure 4B shows a series of optical sections taken from secreting parietal cells simultaneously probed with fluores-

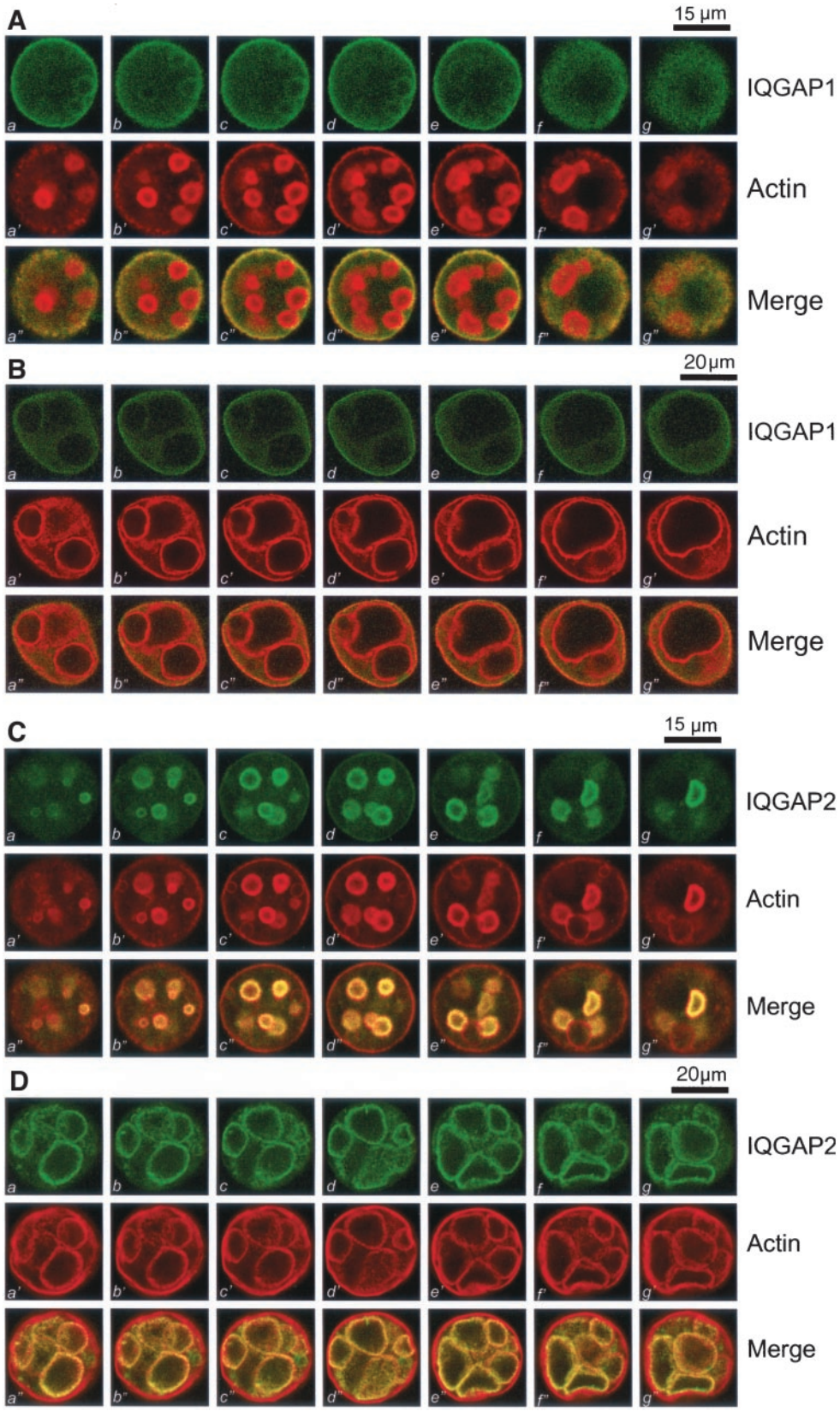

Figure 4. Polarized distribution of IQGAP1 and IQGAP2 in resting and secreting parietal cells. (A) IQGAP1 is preferentially localized to the basolateral membrane of resting parietal cells. This triple montage represents a series of optical sections from the bottom (a, a′, and a″) to the top (h, g′, and g″), of a resting gastric parietal cell doubly stained for IQGAP1 (green, a–g), F-actin (red, a′–g′), and their merges (a″–g″). IQGAP1 is mainly located to basolateral membrane surface and cytoplasm. Somewhat lighter staining of IQGAP1 can also been seen as rings, in a pattern of the suggestive of the invaginations of the apical plasma membrane forming the intracellular canaliculi. Bar, 15 μm. (B) This triple montage of a series of optical sections was arranged in a similar way to that of A, but the parietal cells were stimulated with histamine. Individual images from each focal plane of two fluorophores were collected and processed using Adobe Photoshop. Bar, 20 μm. (C) IQGAP2 is preferentially localized to the apical membrane of the parietal cells. This triple montage of optical sections is arranged similarly to that shown in A, but in this case the resting parietal cells were doubly stained for IQGAP2 (green, a–g), F-actin (red, a′–g′), and merged images. IQGAP2 is chiefly localized to the intracellular of parietal cells, with a distribution profile similar to that F-actin, except for the basolateral surface staining of F-actin. Bar, 15 μm. (D)This triple montage of a series of optical sections was arranged in a similar way to that of C, but in this case the parietal cells were stimulated with histamine. Bar, 20 μm.

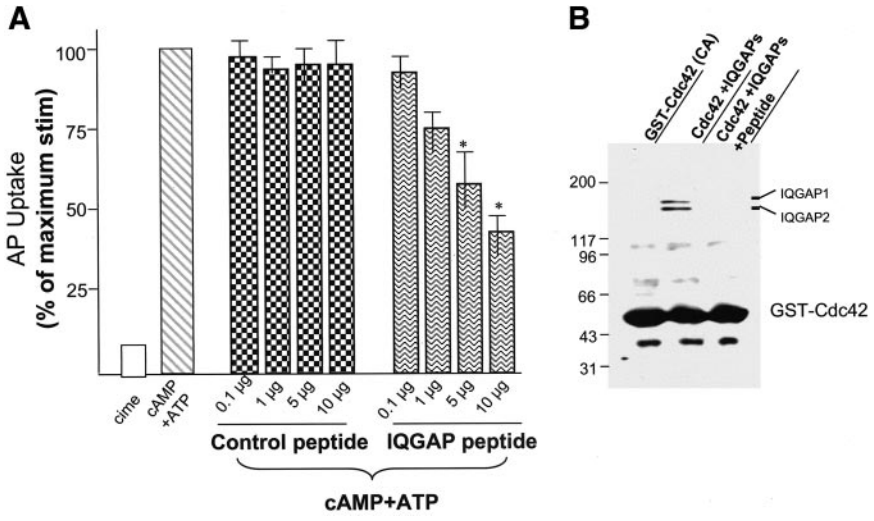

Figure 5. Interaction between Cdc42 and IQGAP2 is essential for parietal cell activation. (A) Synthetic peptides, both inhibitory and scrambled (control), were added into SLO-gland suspensions as indicated amount (micrograms per milliliter). Glands were then stimulated with 100 μM cAMP plus 100 μM ATP, and the AP uptake was measured as described in MATERIALS AND METHODS. AP data are plotted as percentage of the stimulated control for each of experiment. Error bars represent SE; n = 4. *, significant difference compared with stimulated controls ($p < 0.05$). (B) Constitutive active GST-cdc42 proteins coupled to glutathione agarose beads were used to absorb IQGAP proteins followed by incubation of aliquots beads with the inhibitory and scrambled peptide, respectively. Agarose bead-bound proteins were fractionated by SDS-PAGE and stained with Coomassie Blue. Note there are two IQGAP polypeptides were wiped off by 10 μg/ml inhibitory peptide.

cein-labeled anti-IQGAP1 antibody and rhodamine-conjugated phalloidin. Similar to Figure 4A, there was very little coincidence in the distribution of F-actin with that of IQGAP1 near the apical plasma membrane. However, there was some colocalization of F-actin with IQGAP1 toward the basolateral surfaces of parietal cells (Figure 4B, c–e vs. c′–e′). We conclude that IQGAP1 is primarily localized to the basolateral surface of parietal cells.

IQGAP2 Is Mainly Localized to Apical Membrane of Resting and Secreting Parietal Cells

Previous studies suggested that IQGAP2 is a tissue-specific protein restricted to liver cells (Brill *et al.*, 1996). To reveal the subcellular distribution of IQGAP2, we took serial confocal images from double-stained cultured parietal cells, as previously carried out for IQGAP1. Figure 4C shows optical sections from those cells simultaneously probed with monoclonal anti-IQGAP2 antibody (green) and phalloidin (red). In the central region of the cell (Figure 4C, b–g), IQGAP2 staining is clearly visible as rings that outline the apical canalicular membrane. Within parietal cells, IQGAP2 is chiefly colocalized with F-actin with very light staining at the basolateral surface. Also, codistribution of IQGAP2 with F-actin in the apical membrane is apparent as the focal plane moves up and down through the cell. In fact, the overlapping images (yellow, a″–g″) exemplify a superimposition of the two probes in the apical plasma membrane of parietal cells.

Figure 4D shows a series of optical sections taken from identical planes for secreting parietal cells simultaneously stained for IQGAP2 (green) and phalloidin (red). Similar to the earlier staining, F-actin labeling (Figure 4C, a′–g′) outlines the dilated apical plasma membrane. Within parietal cells, IQGAP2 and F-actin are primarily colocalized to the same regions, characteristic of the dilated apical canalicular membrane invaginated into the cytoplasm of parietal cells. Virtually no deposition of IQGAP2 stain can be found at the basolateral surface. Thus, IQGAP2 remains associated with actin cytoskeleton during the expansion of the apical plasma membrane in secreting parietal cells.

*Cdc42*IQGAP2 Interaction Is Necessary for Parietal Cell Activation*

It has been shown that IQGAP proteins bind to active Cdc42 via their GAP domains (Brill *et al.*, 1996). To explore the functional role of the Cdc42*IQGAP interaction in parietal cell activation, we introduced into SLO-glands a synthetic peptide derived from IQGAP proteins, which contains the Cdc42-binding motif. As shown in Figure 5A, addition of such an IQGAP peptide, but not scrambled (control peptide), caused a dose-dependent inhibition of acid secretion as judged by AP uptake, reaching 58.7 ± 4.3% inhibition when the peptide was added at 10 μg/ml (Figure 5A). This effect is specific for the IQGAP peptide, because it was not seen when scrambled (control) peptide was added to SLO-glands (Figure 5A). The disruption of Cdc42*IQGAP interactions in vitro by the IQGAP peptide is shown in Figure 5B. Incubation of the peptide (10 μg/ml) with Cdc42 affinity beads absorbed with IQGAP proteins resulted in a complete removal of IQGAP proteins from the affinity beads, indicating that the IQGAP peptide competes with full-length IQGAP proteins for their association with Cdc42. These studies indicate that interactions between IQGAPs and Cdc42 are important for parietal cell acid secretion.

Both integrity and dynamics of the apical actin cytoskeleton are required for parietal cell activation of secretion (Forte and Yao, 1996). To determine whether the peptide disrupts association between IQGAP proteins and Cdc42 protein in vivo and whether altered IQGAP*Cdc42 interactions prevent the apical membrane dynamics associated with parietal cell activation, we carried out confocal microscopic analyses of parietal cells pretreated with the chimeric TAT-fused peptide followed by histamine stimulation. The inhibition of the TAT-fused peptide on acid secretion in intact cells was found to be equal to that of the IQGAP peptide on SLO-permeabilized cells, whereas efficiency of the TAT-fused peptide across the cell membrane was typically 83 ± 4% as judged by uptake of the FITC-labeled peptide.

As shown in Figure 6A (a′–g′), addition of the peptide did not alter the distribution profile of actin staining. However, the

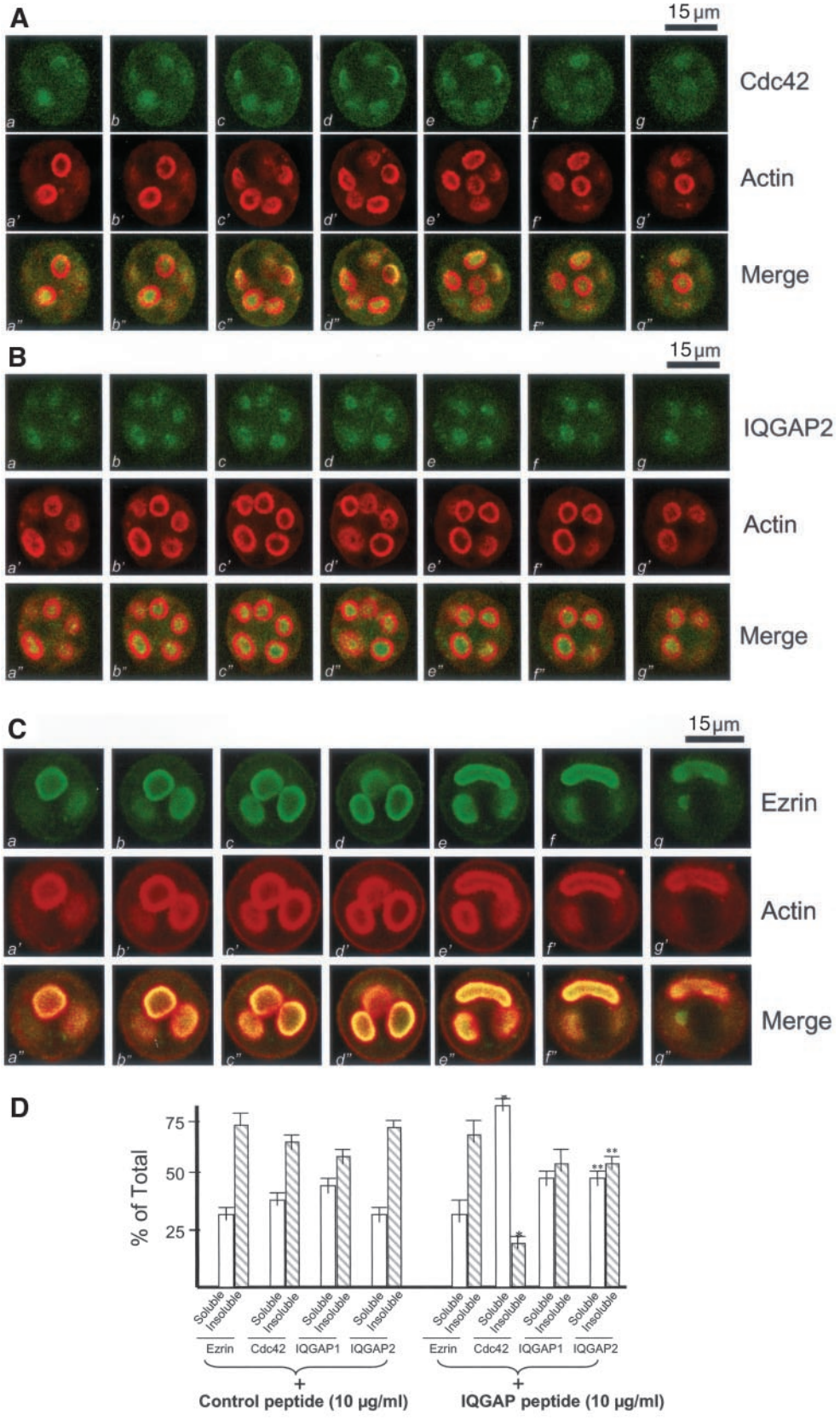

Figure 6. IQGAP2 *Cdc42 interaction is required for the apical membrane remodeling associated with regulated secretion. (A) This triple montage of optical sections is arranged similarly to that shown in Figure 4, but in this case the peptide-treated, histamine-stimulated parietal cells were doubly stained for Cdc42 (green, a–g), F-actin (green, a′–g′), and merged images. Although F-actin is chiefly localized to the apical plasma membranes, the Cdc42 labeling is liberated from the apical vacuoles and diffused throughout the cytoplasm. Individual fluorescent images from each focal plane of two fluorophores were collected and processed using Adobe Photoshop. Bar, 15 μm. (B) This triple montage of a series of optical sections was arranged in a similar way to that of A, but in this case the parietal cells were stained with IQGAP2 and F-actin. It was readily apparent, although F-actin is chiefly localized to the apical plasma membranes, the IQGAP2 labeling is released from the apical vacuoles and diffused throughout the cytoplasm. Bar, 15 μm. (C) This triple montage of a series of optical sections was arranged in a similar way to that of A, but in this case the parietal cells were stained with ezrin and F-actin. It was readily apparent, both ezrin and F-actin remain localized to the apical plasma membranes. Bar, 15 μm. (D) The IQGAP-derived peptide increases the extractable Cdc42 and IQGAP2. Cultured parietal cells were treated with the IQGAP-derived peptide followed by a Triton X-100 extraction. The glandular proteins were separated into a soluble and insoluble fraction as described in MATERIALS AND METHODS. Samples were run on SDS-PAGE, blotted to nitrocellulose, and immunoprobed for ezrin, Cdc42, IQGAP1, and IQGAP2, respectively. The signals were quantified using a PhosphorImager with values expressed as percentage of total (soluble + insoluble). Error bars represent SE; n = 4. Significant difference with respect to the controls (*$p < 0.01$; **$p < 0.05$).

Table 1. IQGAP2*Cdc42 interaction is essential for the apical membrane extension

Treatment	Apical Vacuole Diameter (μm)[a]
Cimetidine	3.9 ± 0.7
Histamine + IBMX	15.9 ± 1.5
Control peptide + histamine + IBMX	15.7 ± 1.7
IQGAP peptide + histamine + IBMX	7.9 ± 1.1*

* $p < 0.01$ compared with those of stimulated cells that were pretreated with the control peptide.

[a] Diameter of apical vacuoles was measured as an index for apical membrane extension associated with acid secretion. Data were obtained from >100 cells in which apical vacuoles were in the same focal plane (see MATERIALS AND METHODS).

optical sections shown in Figure 6A (a–g vs. a′–g′) reveal a drastic difference in the staining patterns between F-actin and Cdc42. Predominantly, Cdc42 staining is seen as a diffuse signal throughout the cytoplasm (Figure 6A, a–g) in the TAT-fused peptide-treated cells. This is readily apparent when the serial images from the two fluorophores are merged (Figure 6A, a″–g″), suggesting that the IQGAP2*Cdc42 interaction is required for a stable localization of Cdc42 to the apical plasma membrane (Table 1), because the TAT-fused scrambled peptide did not alter Cdc42 localization (our unpublished data).

We further examined the distribution profiles of IQGAP1 and IQGAP2 in parietal cells exposed to the TAT-fused peptide. Although there is no apparent alteration of IQGAP1 staining (our unpublished data), the optical sections shown in Figure 6B (a–g vs. a′–g′) reveal distinct distribution profiles between F-actin and the IQGAP2 protein, suggesting that disruption of the Cdc42*IQGAP2 contact altered the localization profile of IQGAP2.

Because ezrin is a major apical cytoskeleton-membrane linker essential for parietal cell activation (Yao *et al.*, 1993; Urushidani *et al.*, 1997), we examined the effect of peptide treatment on ezrin distribution. As shown in Figure 6C, ezrin remains associated with the actin cytoskeleton of apical vacuoles, whereas the peptide liberates Cdc42 and IQGAP2 from the cytoskeleton. This indicates the specificity of the peptide and verifies that there is no direct physical association between ezrin and the Cdc42*IQGAP2 complex (e.g., Figure 3C).

To measure the relative proportion of Cdc42 associated with the cytoskeleton of parietal cells, detergent-soluble and -insoluble fractions were prepared. In accordance with previous studies (Yao *et al.*, 1995), ezrin is mainly found in the Triton X-100–insoluble fraction (73.3 ± 7.1%; Figure 6D, control). As shown in Figure 6D, the nonextractable Cdc42, IQGAP1, and IQGAP2 values in control peptide-treated cells are 64.3 ± 4.9, 58.5 ± 5.1, and 72.9 ± 6.3%, respectively. Interestingly, the TAT-fused IQGAP peptide significantly increased the extractable Cdc42 and IQGAP2 with respect to those of the control peptide (Figure 6D; IQGAP peptide plus). Most of the Cdc42 (81.2 ± 5.1%) is released into the Triton X-100–soluble fraction. In contrast, there was no significant difference in the amount of IQGAP1 and ezrin extracted from control or peptide-treated cells. Thus, we conclude that IQGAP2 links Cdc42 to the apical cytoskeleton of parietal cells.

*Absence of Cdc42*IQGAP2 Interaction Prevents Dilation of Apical Vacuoles*

Because the apical vacuoles dilate upon parietal cell activation, the diameters of the vacuoles can be used as an accurate cytological reporter for judging parietal cell secretion (Agnew *et al.*, 1999). We therefore measured the apical vacuole diameter in >100 parietal cells in which the vacuoles look round and in the same focal plane (Table 1). Control nonsecreting cells exhibited a diameter of 3.9 ± 0.7 μm. Stimulation dramatically extends the diameter to 15.9 ± 1.5, whereas pretreatment of parietal cells with the peptide prevents dilation of the vacuoles. The average vacuole diameter of IQGAP peptide-treated stimulated cells was 7.9 ± 1.1 μm. We conclude that Cdc42*IQGAP2 interactions are essential for dynamic remodeling of the apical cytoskeleton of parietal cells.

DISCUSSION

Cdc42 is a small-molecular-weight GTPase, implicated in a variety of aspects of cellular dynamics. IQGAP1 and IQGAP2 are two types of GAP shown to interact with Cdc42. IQGAP2 was first isolated from liver cells (Brill *et al.*, 1996). In fact, it has been hypothesized that IQGAP2 is a liver tissue-specific GAP protein (McCallum *et al.*, 1996). Herein, we provide the first evidence that Cdc42 is present in gastric parietal cells and is polarized to the apical plasma membrane. Moreover, we offer the novel demonstration that both IQGAPI and IQGAP2 are present in these cells and differentially polarized to the basolateral and apical plasma membranes, respectively. Furthermore, our studies show that Cdc42 interacts with IQGAP2 at the apical membrane of the parietal cells. Finally, we showed that interaction between IQGAP2 and Cdc42 is required for polarized secretion in gastric parietal cells.

A major role for actin cytoskeleton in the secretory processes of parietal cells has been implied from studies by using actin disruptors such as cytochalasin B that disorganize actin filaments within the apical microvilli and act to inhibit acid secretion (Black *et al.*, 1982). Highly organized microfilaments are typical features of microvilli within the parietal cell canaliculus. In going from the resting to secreting state, there are major changes in the apical canalicular surface of parietal cell, including elongation of microvilli. Interestingly, as parietal cells return to the resting state after withdrawal of stimulants, microfilament ultrastructural changes become apparent as a disorganization of actin filaments occurs with collapse of the apical canalicular surface (Forte *et al.*, 1977; Forte and Yao, 1996). These morphological studies indicate that reversible actin-based cytoskeletal dynamics underlie the polarized secretion cycle in parietal cells.

The present studies show that Cdc42 protein is localized to the apical plasma membrane of cultured parietal cells. In addition, we show that activation of Cdc42 is important for acid secretion by parietal cells. However, activation of Cdc42 in the absence of cAMP and ATP did not trigger any acid secretion. The polarized secretion in parietal cells involves

multiple temporally coordinated events, including cAMP-regulated translocation of the proton pump to the apical membrane (Ammar *et al.*, 2002), followed by reorganization of apical cytoskeleton, which facilitates insertion of the pump. Remodeling of the apical membrane cytoskeleton without partition of the proton pump in the apical membrane is not sufficient for parietal cell secretion. However, it would be of great interest to carry out ultrastructural examination as to whether active Cdc42 alone can mimic the histamine-induced reorganization of actin cytoskeleton in parietal cells.

Our data also reveal that IQGAP2 is mainly localized to the apical plasma membrane, which coincides with Cdc42 and actin localization. In addition, Cdc42 binds to both IQGAP1 and IQGAP2 in an activity-dependent manner in our assay, which uses activity-modified mutant proteins (Figure 3). Using GST-Cdc42 (wild-type) protein as an affinity matrix, it has been shown that IQGAP2 binds to Cdc42 in a nucleotide-independent manner (Brill *et al.*, 1996; McCallum *et al.*, 1996). These authors reasoned that IQGAP2 may bind to the regions on Cdc42 that do not undergo conformational change upon GTP hydrolysis. It is possible that the nucleotide-independent IQGAP2-binding regions were altered due to a mutation in the negative, but not active, Cdc42 recombinant protein used in our assay. Alternatively, it is possible that tissue-specific expression of some as yet identified regulators may account for the difference in the requirement of nucleotide hydrolysis for Cdc42*IQGAP2 association observed in previous studies and the present investigation. In any event, it would be of great interest to clarify whether IQGAP2*Cdc42 interactions depend on GTP hydrolysis.

Interestingly, the IQGAP1 protein is predominantly localized to the basolateral plasma membrane of culture parietal cells. A similar polarized distribution pattern has been reported for cytoplasmic β- and γ-actin isoforms (Yao *et al.*, 1995). It should be pointed out that the spatial separation of IQGAP1 and IQGAP2 is not absolute. Very faint basolateral staining indicating IQGAP2 was also observed by using IQGAP2 antibody, and we occasionally observed a low level of IQGAP1 staining within the apical plasma membrane, although basolateral staining was overwhelming. In addition, some cytoplasmic staining of both IQGAP1 and IQGAP2 was observed.

Besides a polarized distribution of the cytoplasmic β- and γ-actin isoforms, we previously showed that ezrin is also polarized to the apical membrane and colocalized with the cytoplasmic β-actin isoform (Yao *et al.*, 1995, 1996a). The preferential association between ezrin and the cytoplasmic β-actin isoform was reconstituted in a test tube assay where purified ezrin from parietal cells was shown to selectively bind to cytoplasmic β-actin isolated from red blood cells, but not skeletal muscle actin isoform (Yao *et al.*, 1996a). Interestingly, LASP-1, a 40-kDa cAMP-dependent phosphoprotein, was also shown to be polarized to the basolateral membrane in resting parietal cells (Chew *et al.*, 2000). Liberation of ezrin from apical actin microvilli by ME3407, a PI3 kinase inhibitor, was correlated to the inability of parietal cells to secrete (Urushidani *et al.*, 1997). In addition, selective loss of full-length ezrin by calpain-mediated proteolysis inhibited parietal cell secretion (Yao *et al.*, 1993). From these examples, it is clear that the integrity of the actin-based cytoskeleton of apical microvilli plays a very important role in regulated acid secretion. Polarized delivery and incorporation of proteins and lipids to specific domains of the plasma membrane is fundamental to a wide range of biological processes such as neuronal synaptogenesis and epithelial cell polarization. The preferential distribution of actin isoforms together with their accessory proteins, such as ezrin, LASP-1, IQGAP1 and IQGAP2 shown herein, provide a molecular basis accounting for cell polarity in gastric parietal cells and perhaps in other epithelial cells.

Our studies presented herein show that IQGAP2 provides a link between Cdc42 and the apical cytoskeleton of the parietal cells. The IQGAP-derived peptide disrupts Cdc42*IQGAP2 association and liberates Cdc42 from the cytoskeleton. This relocation of Cdc42 coincided with inhibition of acid secretion in parietal cells. However, disruption of the Cdc42*IQGAP2 protein complex did not abolish parietal cell secretion, suggesting that a Cdc42-independent pathway may also be involved in parietal cell activation. In fact, the loss of Cdc42 from the apical cytoskeleton did not alter the localization of ezrin, an actin-binding protein essential for parietal cell activation. Mackay *et al.* (1997) reported that ezrin/radixin/moesin proteins interact with Rho and Rac in the assembly of focal adhesion complexes and actin filaments in fibroblasts. It would be of great interest to elucidate how the Cdc42-independent pathway cross talks with the Cdc42-dependent cascade in regulated epithelial cell secretion.

Taken together, our present work reveals for the first time that IQGAP1 and IQGAP2 coexist differentially in gastric epithelial cells, in a polarized distribution pattern. IQGAP2 predominates in the secretory canaliculus of parietal cells, whereas IQGAP1 is concentrated near basolateral membrane sites with diminished localization to the secretory canaliculi. Moreover, the subcellular distribution profile of IQGAP2 closely superimposes on that of Cdc42 (to the apical plasma membrane), whereas the subcellular distribution profile of IQGAP1 is largely dissimilar, being localized to the basolateral membrane. Finally, we show that IQGAP2 interacts with Cdc42 at the apical cytoskeleton of gastric parietal cells and that such interaction is required for parietal cell secretion. Given the preferential interaction between IQGAP2 and Cdc42 established herein, we propose that IQGAP2 links Cdc42 to the actin-based cytoskeleton at the apical plasma membrane and facilitates the apical cytoskeletal dynamics required for polarized secretion in epithelial cells.

ACKNOWLEDGMENTS

We thank Dr. John Forte for continuous support and advice, Dr. Alan Hall for the Cdc42 cDNA constructs, and Dr. David King for peptide synthesis. We also thank members of Drs. Forte's and Machen's groups for insightful discussion during the course of this study. This work was supported by grants from Chinese Outstanding Young Scientist Award (39925018), Chinese Academy of Science (KSCX2-2-01), National Institutes of Health (DK-56292), and American Cancer Society (RPG59282) to X.Y. X.Y. is an Industrial Research Scholar of American Digestive Health Foundation, and Cheung Kong Scholar of Li Ka Shing Foundation.

REFERENCES

Agnew, B.J., Duman, J.G., Watson, C.J., Coling, D.J., and Forte, J.G. (1999). Cytological transformations associated with parietal cell stimulation: critical steps in the activation cascade. J. Cell Sci. *112*, 2639–4266.

Ammar, D.A., Zhou, R., Forte, J.G., and X. Yao. (2002) Syntaxin 3 is required for cAMP-induced acid secretion. streptolysin O-permeabilized gastric gland model. Am. J. Physiol. *282*, G23–G33.

Bishop, A.L., and Hall, A. (2000). Rho GTPases, and their effector proteins. Biochem. J. *348*, 241–256.

Black, J.A., Forte, T.M., and Forte, J.G. (1982). The effects of microfilament disrupting agents on HCl secretion and ultrastructure of piglet gastric oxyntic cells. Gastroenterology *83*, 595–604.

Brill, S., Li, S., Lyman, C.W., Church, D.M., Wasmuth, J.J., Weissbach, L., Bernards, A., and Snijders, A.J. (1996). The ras GTPase-activating-protein-related human protein IQGAP2 harbors a potential actin binding domain and interacts with calmodulin and Rho family GTPases. Mol. Cell. Biol. *16*, 4869–4878.

Chen, Y.N., Sharma, S.K., Ramsey, T.M., Jiang, L., Martin, M.S., Baker, K., Adams, P.D., Bair, K.W., and Kaelin, W.G. Jr. (1999). Selective killing of transformed cells by cyclin/cyclin-dependent kinase 2 antagonists. Proc. Natl. Acad. Sci. USA *96*, 4325–4329.

Chew, C.S. (1985). Parietal cell protein kinases. Selective activation of type I cAMP-dependent protein kinase by histamine. J. Biol. Chem. *260*, 7540–7550.

Chew, C.S., Parente, J.A. Jr., Chen, X., Chaponnier, C., and Cameron, R.S. (2000). The LIM, and SH3 domain-containing protein, lasp-1, may link the cAMP signaling pathway with dynamic membrane restructuring activities in ion transporting epithelia. J. Cell Sci. *113*, 2035–2045.

Drubin, D.G., and Nelson, W.J. (1996). Origins of cell polarity. Cell *84*, 335–344.

Erickson, J.W., Cerione, R.A., and Hart, M.J. (1997). Identification of an actin cytoskeletal complex that includes IQGAP and the Cdc42 GTPase. J. Biol. Chem. *272*, 24443–24447.

Feig, L. (1999). Tools of the trade: use of dominant-inhibitory mutants of Ras-family GTPases. Nat. Cell Biol. *1*, E25–E27.

Forte, J.G., Black, J.A., Forte, T.M., Machen, T.E., and Wolosin, J.M. (1981). Ultrastructural changes related to functional activity in gastric oxyntic cells. Am. J. Physiol. *241*, G349–G358.

Forte, T.M., Machen, T.E., and Forte, J.G. (1977). Ultrastructural changes in oxyntic cells associated with secretory function: a membrane-recycling hypothesis. Gastroenterology *73*, 941–955.

Forte, J.G., and Yao, X. (1996). The Membrane-recruitment-and-recycling hypothesis of gastric HCl secretion. Trends Cell Biol. *6*, 45–48.

Fukata, M., T. Watanabe, J. Noritake, M. Nakagawa, M. Yamaga, S. Kuroda, Y. Tatsuura, A. Iwamatsu, F. Perez, and Kaibuchi, K. (2002). Rac1 and Cdc42 capture microtubules through IQGAP1 and CLIP-170. Cell *109*, 873–885.

Guo, W., Roth, D., Walch-Solimena, C., and Novick, P. (1999). The exocyst is an effector for Sec4p, targeting secretory vesicles to sites of exocytosis. EMBO J. *18*, 1071–1081.

Hall, A. (1998). Rho GTPases and the actin cytoskeleton. Science *279*, 509–514.

Hart, M.J., Callow, M.G., Souza, B., and Polakis, P. (1996). IQGAP1, a calmodulin-binding protein with a rasGAP-related domain, is a potential effector for cdc42Hs. EMBO J. *15*, 2997–3005.

Helander, H.F., and Sundell, G.W. (1984). Ultrastructure of inhibited parietal cells in the rat. Gastroenterology *87*, 1062–1071.

Joyal, J.L., Annan, R.S., Ho, Y., Huddleston, M.E., Carr, S.A., Hart, M.J., and Sacks, D.B. (1997). Calmodulin activates phosphatidylinositol 3-kinase. J. Biol. Chem. *272*, 15419–15428.

Kuroda, S., Fukata, M., Kobayashi, K., Nakafuku, M., Nomura, N., Iwamatsu, A., and Kaibuchi, K. (1996). Identification of IQGAP as a putative target for the small GTPases, Cdc42 and Rac1. J. Biol. Chem. *271*, 23363–23367.

Li, S., Wang, Q., Chakladar, A., Bronson, R.T., and Bernards, A. (2000). Gastric hyperplasia in mice lacking the putative Cdc42 effector IQGAP1. Mol. Cell Biol. *20*, 697–701.

Mackay, D.J., Esch, F., Furthmayr, H., and Hall, A. (1997). Rho- and Rac-dependent assembly of focal adhesion complexes and actin filaments in permeabilized fibroblasts: an essential role for ezrin/radixin/moesin proteins. J. Cell Biol. *138*, 927–938.

McCallum, S.J., Wu, W.J., and Cerione, R.A. (1996). Identification of a putative effector for Cdc42Hs with high sequence similarity to the RasGAP-related protein IQGAP1 and a Cdc42Hs binding partner with similarity to IQGAP2. J. Biol. Chem. *271*, 21732–21737.

Rosenfeld, J., Capdevielle, J., Guillemot, J.C., and Ferrara, P. (1992). In-gel digestion of proteins for internal sequence analysis after one- or two-dimensional gel electrophoresis. Anal. Biochem. *203*, 173–179.

Urushidani, T., Muto, Y., Nagao, T., Yao, X., and Forte, J.G. (1997). ME-3407, a new antiulcer agent, inhibits acid secretion by interfering with redistribution of H(+)-K(+)-ATPase. Am. J. Physiol. *272*, G1122–G1134.

Verdecia, M.A., Bowman, M.E., Lu, K.P., Hunter, T. and Noel, J.P. (2000). Structural basis for phosphoserine-proline recognition by group IV WW domains. Nat. Struct. Biol. *8*, 639–643.

Weissbach, L., Settleman, J., Kalady, M.F., Snijders, A.J., Murthy, A.E., Yan, Y.X., and Bernards, A. (1994). Identification of a human rasGAP-related protein containing calmodulin-binding mot. J. Biol. Chem. *269*, 20517–20521.

Yao, X., and Forte, J.G. (2003). Cell biology of acid secretion by the parietal cell. Annu. Reb. Physiol. *65*, 103–131.

Yao, X., Anderson, K.L., and Cleveland, D.W. (1997). The microtubule-dependent motor CENP-E is an integral component of kinetochore corora fibers that link centromeres to spindle microtubules. J. Cell Biol. *139*, 435–447.

Yao, X., Chaponnier, C., Gabbiani, G., and Forte, J.G. (1995). Polarized distribution of actin isoforms in gastric parietal cells. Mol. Biol. Cell *6*, 541–557.

Yao, X., Cheng, L., and Forte, J.G. (1996a). Biochemical characterization of ezrin-actin interaction. J. Biol. Chem. *271*, 7224–7229.

Yao, X., Karam, S.M., Ramilo, M., Rong, Q., Thibodeau, A., and Forte, J.G. (1996b). Stimulation of gastric acid secretion by cAMP in a novel α-toxin-permeabilized gland model. Am. J. Physiol. *271*, C61–C73.

Yao, X, Thibodeau, A., and Forte, J.G. (1993). Ezrin-calpain I interactions in gastric parietal cells. Am. J. Physiol. *265*, C36–C46.

Zhang, J., Fu, C., Miao, Y., Duo, Z., and Yao, X. (2002). Protein kinase TTK interacts and co-localizes with CENP-E to the kinetochore of human cells. Sci. Bull. *27*, 213–219.

Zhang, X., Bi, E., Novick, P., Du, L., Kozminski, K.G., Lipschutz, J.H., and Guo, W. (2001). Cdc42 interacts with the exocyst and regulates polarized secretion. J. Biol. Chem. *276*, 46745–46750.